Thermal Transfer in Turbulent Gas Streams: Temperature Distribution in Boundary Flows About Spheres

L. N. BATHISH and B. H. SAGE

California Institute of Technology, Pasadena, California

A knowledge of the temperature distribution about bodies of revolution, and more particularly about spheres, is of interest in connection with many problems associated with thermal and material transport. The present investigation involved measurements of the temperature distribution in the boundary flows about a 0.5-in. porous sphere and 0.5-in. and 1.0-in. silver spheres. The measurements were made in an air stream at velocities between 4 and 32 ft./sec. under conditions of shear flow, as well as at various positions in the wake of a perforated grid. From these measurements the thickness of the thermal boundary layer was established as a function of polar angle and conditions of flow. The experimental data were correlated upon the assumption that the normalized temperature in the boundary flow is a single-valued function of the position in the thermal boundary layer. It appeared that this simple assumption described the experimental data within the uncertainties of measurement and that the Blasius function provided a reasonable description of the relationship of the normalized temperature to the relative position in the thermal boundary layer.

The gross thermal transport to spheres has been the subject of many experimental studies. Much of the older work was summarized ably by McAdams (*16*). Experimental studies have been made by Tang (*23*) and Johnstone (*13*), and more recently Sato (*18*) and Brown (*2*) investigated experimentally the thermal and material transfer from spheres in turbulent air streams. These data all indicate a marked influence of the apparent level of turbulence upon thermal and material transport. It appears that the influence of apparent level of turbulence is more pronounced in the case of combined thermal and material transport than in the case of thermal transport alone (*2*).

Local thermal transport from spheres has been investigated to a much more limited extent. The measurements of Cary (*4*), Lautman (*15*), Xenakis (*25*), and Wadsworth (*24*) have been supplemented by the work of Hsu (*11*) and Short (*20*), who established the local thermal transport by measurement of the temperature gradients in the air stream surrounding a sphere.

A review of the theoretical investigations of thermal transport in the three-dimensional boundary flows encountered around spheres was made by Hsu (*11*). Sibulkin (*22*), Korobkin (*14*), Frössling (*10*), Eckert (*9*), and Drake (*8*) have all contributed to an understanding of the prediction of the local thermal transport around spheres. Each approach appears however to be subject to limiting assumptions and can be considered only an approximation for prediction of the local thermal transport. For this reason further information concerning the temperature distribution in boundary flows appeared worthwhile.

The present experimental program was undertaken for the purpose of evaluating the temperature distribution around spheres. The study involved evaluation from experimental data of the thermal boundary-layer thickness as a function of polar angle, level of turbulence, and Reynolds number. An earlier study (*11*) presented limited experimental information covering macroscopic and local transport from spheres and also attempted to relate the temperature distribution in the boundary flows to the thermal boundary-layer thickness. The present study involves a marked extension of the earlier experimental work, and the methods and techniques employed were refinements of those used earlier. Experimental data were obtained upon both a 0.5- and 1.0-in. silver sphere and a 0.5-in. porous ceramic sphere in an air stream at velocities up to 32 ft./sec. Measurements for the silver sphere relate to thermal transport only. Studies with the porous sphere involved the evaporation of *n*-heptane into an air stream and relate to both thermal and material transport.

METHODS AND EQUIPMENT

Descriptions of the spheres (*2, 11, 18*) and of the air supply equipment (*12*) are available. The transverse level of turbulence in the undisturbed air stream was approximately 0.013 root-mean-square fluctuating velocity relative to the average velocity of the stream. The level of turbulence was varied by introducing a perforated plate to the air stream and carrying out measurements at several distances downstream from the plate (*18*). The plate was provided with 0.875-in. holes on 1-in. centers. The longitudinal turbulence in the wake, which was estimated from the measurements of Davis (*6, 7*), has been presented (*18, 20*) and is not included here. Because of uncertainties in the direct applicability of Davis' data the results of this study are presented for distances downstream from the perforated plate. In addition the apparent level of turbulence is indicated.

The temperature distribution around the sphere suspended in an air stream was determined by means of horizontal and vertical traverses. Nine traverses were usually made under each set of conditions. Platinum, platinum-rhodium thermocouples 0.0003 and 0.001 in. in diameter, mounted horizontally, were used.

The position of the horizontal thermocouple relative to the surface of the sphere was known within 0.001 in. The temperature of the thermocouple was determined within 0.02°F. relative to the international platinum scale. Fluctuations in air temperature in the boundary flows were of the order of 0.05°F., except in the wake where fluctuations of as much as 0.2°F. were encountered as a result of vortex rings being shed by the sphere.

The actual thermocouple junction for the thermocouples of both sizes was approximately 0.001 in. in diameter. In the

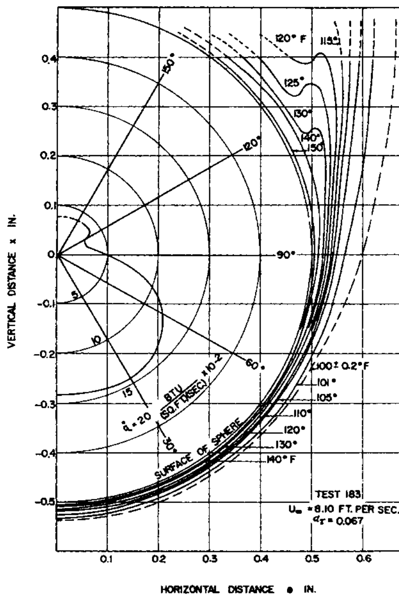

Fig. 1. Wire temperature distribution about a 1.0-in. silver sphere.

case of the 0.001-in. thermocouple a relatively uniform section across the junction was obtained. In the case of the 0.0003-in. thermocouple an irregular spherical mass approximately 0.001 in. in diameter was obtained. Efforts to achieve a uniform section with the smaller thermocouple were not successful.

Careful attention has been given to the errors introduced in measuring the temperature of fluids in the boundary flow about spheres (*21*). In certain instances a significant difference exists between the temperature of the fluid and that of the thermocouple junction. Data presently available concerning the velocity distribution about spheres (*10*) does not describe the local velocities adequately enough to permit the prediction of the transfer from

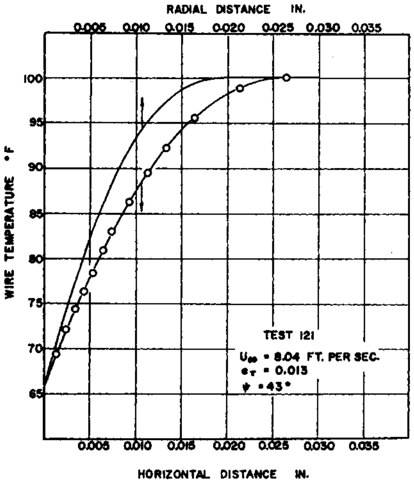

Fig. 2. Horizontal temperature traverse near a 0.5-in. porous sphere.

the wire as a function of position in the boundary flow (*21*). Therefore in the present consideration the wire temperature, defined in this paper as the temperature of the thermocouple junction, was employed as representative of the normalized temperature distribution in the boundary flow. Use of the wire temperature is considered satisfactory because of agreement between the data obtained with the 0.0003- and the 0.001-in. thermocouples. Further, the normalization used here minimizes the influence of differences between the temperature of the fluid at a point and the temperature registered by the thermocouple junction when occupying the same space.

ANALYSIS

The method employed to relate the temperature distribution around a sphere to the conditions of flow involved in principle only the normalization of the temperature in the boundary flow and expression of the radial position as a fraction of the thermal boundary-layer thickness. The temperature, as measured by a thermocouple in the boundary flow, was normalized by means of the following relation:

$$\Upsilon_W = \frac{t_\infty - t_W}{t_\infty - t_{W,i}} \tag{1}$$

The thermal boundary layer thickness was established from

$$\delta_t = \int_{n=0}^{n=\infty} \Upsilon_W \, dn \tag{2}$$

An empirical expression, based on a function proposed by Frössling (*10*) for three-dimensional boundary flow about a sphere, was considered as a frame of reference:

$$\Upsilon = 1 - f_1'(\eta) = 1 - f_1'\left(C\frac{n}{\delta_t}\right) \tag{3}$$

Values of $f_1'(\eta)$ are available (*19*). It was found that Equation (3) did not

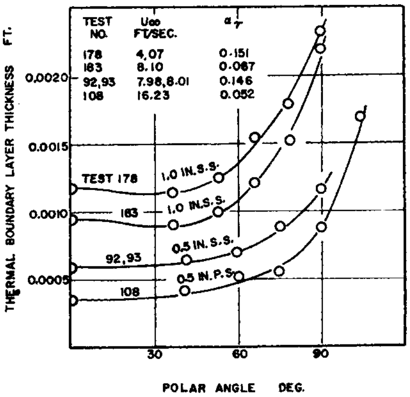

Fig. 3. Effect of polar angle upon thickness of thermal boundary layer.

yield as satisfactory agreement with the experimental data as was obtained with a related empirical expression based on the Blasius function for the velocity distribution along a flat plate (*3*):

$$\Upsilon_W = 1 - f'(\eta) = 1 - f'\left(C\frac{n}{\delta_t}\right) \tag{4}$$

Values of $f'(\eta)$ are available (*5, 19*). It is not clear to the authors why the frame of reference based on the Blasius function proved to be more useful than that based on Frössling's approximation of the three-dimensional boundary flow about a sphere. Equation (4) indicates the normalized temperature Υ_W should be a single-valued function of the relative position in the thermal boundary layer n/δ_t. Such behavior is predicted to a first-order approximation by the integral solution to the boundary flow (*17*).

In reducing the experimental data the standard error of estimate was used as a measure of the deviation of the experimental data from the smoothed curves or smoothed tabular data:

$$\sigma_\Upsilon = \left[\frac{\sum_1^N [(\Upsilon_W)_e - (\Upsilon_W)_{C=1.75}]^2}{N-1}\right]^{1/2} \tag{5}$$

In addition the average deviations both with and without regard to sign were employed:

$$S_\Upsilon = \frac{\sum_1^N [(\Upsilon_W)_e - (\Upsilon_W)_{C=1.75}]}{N} \tag{6}$$

$$S'_\Upsilon = \frac{\sum_1^N \left|[(\Upsilon_W)_e - (\Upsilon_W)_{C=1.75}]\right|}{N} \tag{7}$$

The Reynolds number was evaluated from

$$N_{Re_\infty} = \frac{d\,U_\infty}{\nu_\infty} \tag{8}$$

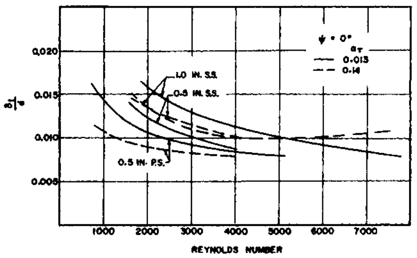

Fig. 4. Normalized thickness of thermal boundary layer at stagnation as a function of Reynolds number.

The foregoing definitions are in accord with standard practice. They are included only to make certain the meaning of the terms employed.

EXPERIMENTAL RESULTS

The present investigation involved fifteen tests with a 0.5-in. silver sphere, eighteen tests with a 0.5-in. porous sphere, and ten tests with a 1.0-in. silver sphere. The experimental conditions relating to the tests are available in tabular form (*1*). The conditions include gross air velocities of 4, 8, 16, and 32 ft./sec. and apparent turbulence levels, as established from the measurements of Davis (*6, 7*), between 0.013 and 0.15. The temperature of the air stream was approximately 100°F. The air-stream pressure and humidity is given in the tabular material for each test. For most of the tests the number of experimental points involved was between 50 and 90.

Figure 1 shows a typical distribution of wire temperature around the 1.0-in.

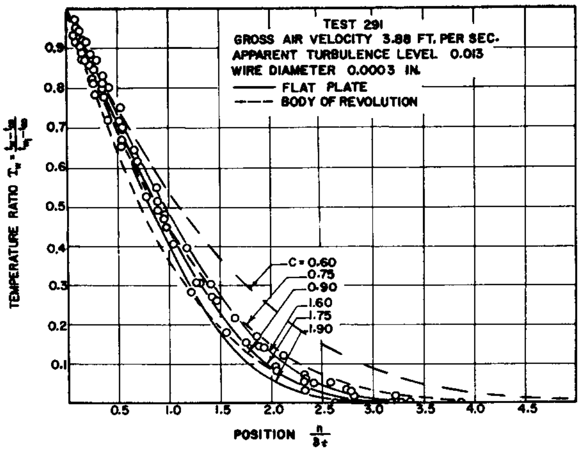

Fig. 5. Comparison of normalized wire temperature in boundary flow with predicted values for a 0.5-in. porous sphere.

silver sphere. The local thermal transport as determined from the temperature gradient at the surface of the sphere is included in the figure. The detail with which the experimental data were obtained is illustrated by the traverse shown in Figure 2. It was necessary to correct the horizontal traverses to corresponding radial traverses at the same polar angle. Usually eight horizontal traverses, such as the one illustrated in Figure 2, and one vertical traverse at stagnation were made for each set of flow conditions investigated.

The experimental information relating to the traverse shown in Figure 2 is available in a table (*1*) which gives the horizontal distance from the sphere, the corresponding radial distance, the wire temperature, the normalized wire temperature, and the relative position in the thermal boundary layer. The thermal boundary-layer thickness as evaluated by the graphical solution in Equation (2) was 0.000476 ft. (*1*).

All the experimental data, of which the data relating to Figure 2 are an example, were smoothed with respect to Reynolds number, apparent level of turbulence, and polar angle. The results of the smoothing operation are recorded in tabular material (*1*) which gives the thermal boundary-layer thickness as a function of Reynolds number and apparent turbulence level for polar angles of 0, 30, 60, and 90 deg., measured from the stagnation point. All the values of thermal boundary-layer thickness reported (*1*) are based upon measurements obtained with the 0.0003-in. platinum, platinum-rhodium thermocouples. The standard error of estimate of the experimental data from the smoothed data is 0.1089 x 10^{-3} ft. for the 0.5-in. silver sphere, 0.0266 x 10^{-3} ft. for the 0.5-in. porous sphere, and 0.0484 x 10^{-3} ft. for the 1.0-in. silver sphere (*1*). In arriving at the standard error of estimate it was assumed that all the uncertainty lay in the thermal boundary-layer thickness and none in the polar angle or conditions of flow.

Figure 3 shows the thickness of the thermal boundary layer as a function of polar angle for four conditions of flow. Data for each of the three spheres are included. The much greater boundary-layer thickness for the 1.0-in. silver sphere is clearly evident. With this sphere the thermal boundary-layer thickness decreases slightly, with increase in polar angle, to a minimum at approximately 45 deg. It then increases rapidly. As would be expected a significant decrease in boundary-layer thickness occurs with increase in velocity for both the 0.5- and 1.0-in. spheres. Furthermore at comparable velocities the boundary-layer thickness for the 0.5-in. silver sphere is much smaller than for the 1.0-in. sphere.

The data of Figure 3 were generalized, on the basis of a simple linearization with respect to the sphere diameter, for the thickness of the thermal boundary layer at stagnation, and the results are shown in Figure 4. The thermal boundary-layer thickness at stagnation appears distinctly smaller when both thermal and material transport are involved than when thermal transport alone occurs. It is not surprising that the effect of apparent level of turbulence differs in the case of the 1.0- and the 0.5-in. silver sphere. The scale of the turbulence induced by the grid is the same in the two cases, and it is entirely probable that the effects on the different sized spheres are different. In any event it appears that at the high Reynolds numbers the stagnation boundary-layer thickness is greater for situations involving a higher apparent level of turbulence. In the case of the 0.5-in. silver sphere this appears to apply at all the Reynolds numbers investigated. In the case of the 1.0-in. sphere it applies only at Reynolds numbers above 5,000. It should be remembered that for the 0.5-in. silver sphere a Reynolds number of 2,500 corresponds to the same actual velocity of the approaching stream as a Reynolds number of 5,000 for the 1.0-in. sphere. The reason that the stagnation boundary-layer thickness

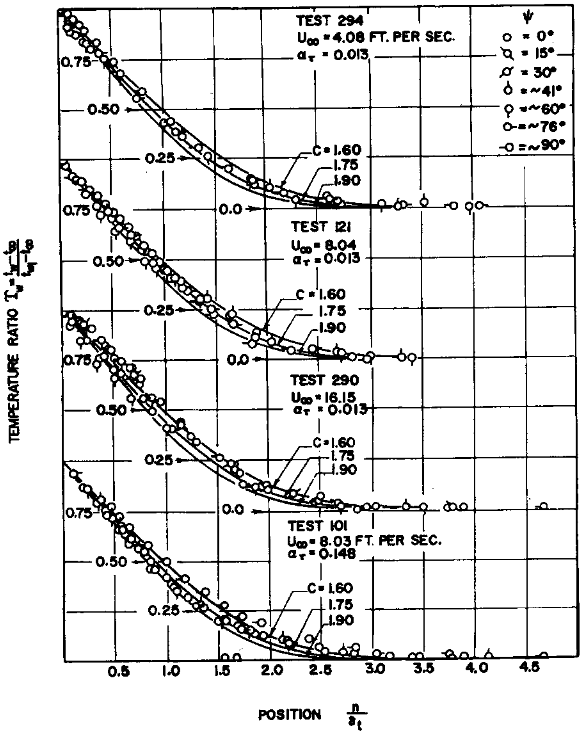

Fig. 6. Normalized wire temperature in boundary flow for a 0.5-in. porous sphere.

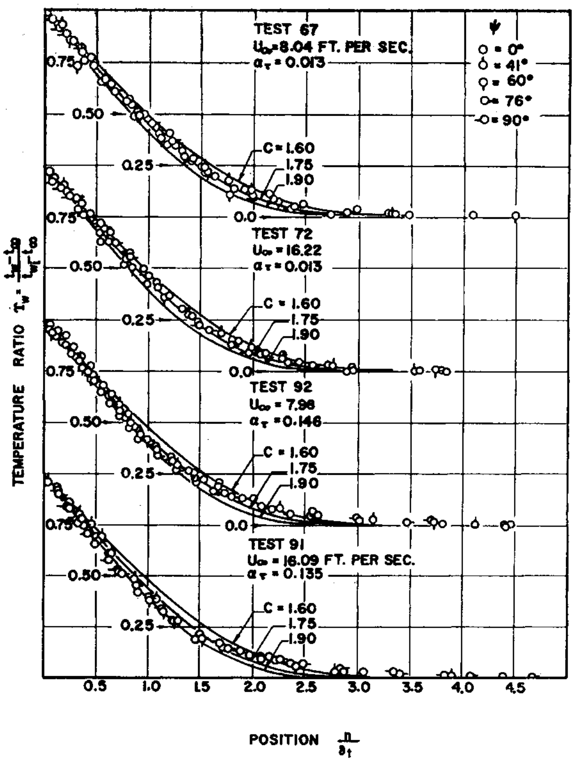

Fig. 7. Normalized wire temperature in boundary flow for a 0.5-in. silver sphere.

for the porous sphere, involving both material and thermal transfer, is smaller at the higher apparent level of turbulence than at the lower, at Reynolds numbers at least up to 5,000, is not clear. This behavior is contrary to the behavior with the 0.5-in. silver sphere.

If it is assumed that Equation (4) is applicable, it follows that the normalized wire temperature, or temperature ratio, should be a single-valued function of the relative position in the thermal boundary layer n/δ_t. All the experimental data were smoothed upon this assumption, and the standard errors of estimate and average deviations of the smoothed data are available (*1*). In evaluating the standard errors of estimate and average deviations it was assumed that all the uncertainty was in the normalized temperature and none in the relative position in the thermal boundary layer. All the data for a single sphere were treated, by necessity, as deviating from a single smoothed curve.

Figure 5 shows the predictions from the function shown in Equation (3) for a body of revolution and from the function in Equation (4) for a flat plate in comparison with experimental data for one set of conditions. It is apparent that the functional relation for a flat plate given in Equation (4) is much more applicable than that for a body of revolution. This was true for all the data. Furthermore use of a value of the coefficient C of 1.75 yielded reasonable agreement with the experimental data. Table 1 records the predicted normalized wire temperature based upon Equation (4), with a value of the coefficient C of 1.75, as a function of relative position in the thermal boundary layer. For comparison the experimental values for the three spheres are included. The standard deviation and the average error with and without regard to sign are included for each sphere. Figure 6 depicts the effect of relative position in the thermal boundary layer upon the normalized wire temperatures obtained in the boundary flows of the 0.5-in. porous sphere. The influence of polar angle is indicated. These data show little systematic variation with conditions of flow. Similarly Figure 7 shows the normalized wire temperature as a function of relative position in the thermal boundary layer for the 0.5-in. silver sphere. Again there is little systematic variation with conditions of flow. The experimental conditions chosen for illustration are typical of those encountered in this study.

Figure 8 presents a comparison for the three spheres of the normalized wire temperatures as a function of relative position in the thermal boundary layer. There is little to choose between the several sets of data. In Figures 6, 7, and 8 the curves corresponding to the functional relationships shown in Equation (4) with values of the coefficient C of 1.60, 1.75, and 1.90 are included. The information in these figures, together with the data presented in Figure 5, illustrates that the simple functional relation set forth by Equation (4) permits a reasonable description of the temperature variations in the boundary flows about a sphere, as long as information concerning the thermal boundary-layer thickness is available. At the present time it is not entirely clear what the influence is of the several variables upon the thermal boundary-layer thickness which is depicted in Figures 3 and 4. In any event

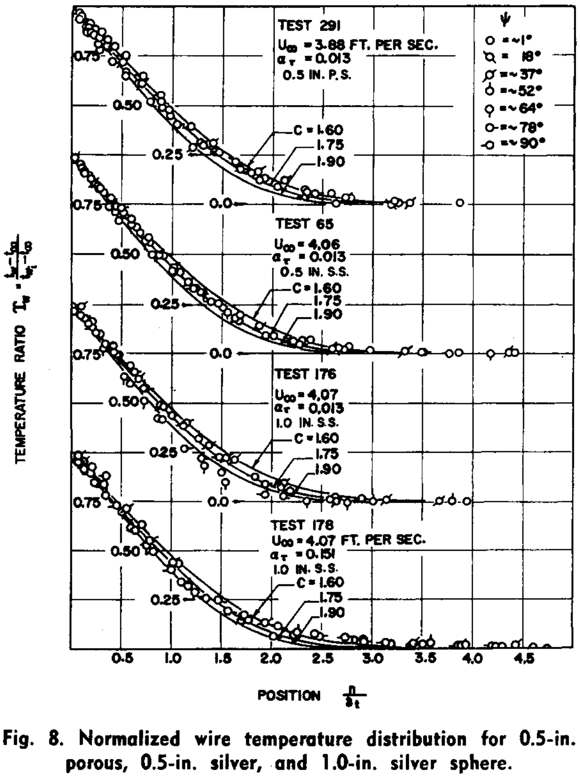

Fig. 8. Normalized wire temperature distribution for 0.5-in. porous, 0.5-in. silver, and 1.0-in. silver sphere.

TABLE 1. NORMALIZED WIRE TEMPERATURES AS A FUNCTION OF POSITION IN THERMAL BOUNDARY LAYER

		Experimental[b]		
Position	Predicted[a]	Porous[c] sphere 0.5 in.	Silver[d] sphere 0.5 in.	Silver[d] sphere 1.0 in.
0	1.000	1.0000	1.0000	1.0000
0.05	0.972	0.9748	0.9697	0.9771
0.10	0.940	0.9428	0.9377	0.9451
0.15	0.914	0.9168	0.9117	0.9191
0.20	0.882	0.8848	0.8797	0.8871
0.25	0.854	0.8568	0.8517	0.8591
0.30	0.822	0.8248	0.8197	0.8271
0.35	0.797	0.7998	0.7947	0.8021
0.40	0.767	0.7698	0.7647	0.7721
0.45	0.738	0.7408	0.7357	0.7431
0.50	0.711	0.7138	0.7087	0.7161
0.60	0.654	0.6568	0.6517	0.6591
0.70	0.598	0.6008	0.5957	0.6031
0.80	0.524	0.5268	0.5217	0.5291
0.90	0.490	0.4928	0.4877	0.4951
1.00	0.440	0.4428	0.4377	0.4451
1.50	0.220	0.2228	0.2177	0.2251
2.00	0.088	0.0908	0.0857	0.0931
2.50	0.026	0.0288	0.0237	0.0311
3.00	0.004	0.0068	0.0017	0.0091
	Standard Error of Estimate =	0.0380	0.0241	0.0262
	Average Deviation (sign) =	0.0028	−0.0023	0.0051
	Average Deviation (no sign) =	0.0282	0.0181	0.0201

[a] Based upon Equation (4) with a value of C of 1.75.
[b] Measured with 0.0003-in. thermocouple.
[c] Boundary flow involves both thermal and material transfer.
[d] Boundary flow involves thermal transfer only.

there appears to be little need to investigate in detail the form of the thermal boundary layer, since the relatively simple prediction set forth by Equation (4) appears to be a reasonable description of the behavior.

ACKNOWLEDGMENT

The assistance of N. T. Hsu and Kazuhiko Sato in connection with the experimental measurements reported here is acknowledged. The Fluor Corporation contributed to this program as donors of the Peter E. Fluor Fellowship to N. T. Hsu. Virginia Berry and Lorine Faris assisted in the reduction of experimental data, and Ann Taylor contributed to preparation of the manuscript.

NOTATION

C = coefficient
d = differential operator
d = diameter of sphere, in. or ft.
f' = Blasius function
f_1' = Frössling function
N = number of experimental points
N_{Re_∞} = free stream Reynolds number, defined in Equation (8)
n = distance normal to surface of the sphere, in. or ft.
$\dot{q}$ = local thermal transport, B.t.u./(sq.ft.)(sec.)
S_{Υ} = average deviation in normalized temperature, defined in Equation (6)
S'_{Υ} = average deviation in normalized temperature, without regard to sign, defined in Equation (7)
t = temperature, °F.
U = velocity, ft./sec.
x, z = coordinate axes with origin at center of sphere, in. or ft.

Greek Letters

α_τ = apparent level of turbulence (fractional)
δ_t = thermal boundary layer thickness, ft.
η = Blasius parameter
ν = kinematic viscosity, sq.ft./sec.
σ_{Υ} = standard error of estimate of normalized temperature defined in Equation (5)
Υ = normalized temperature
Ψ = polar angle, measured from stagnation point, deg.

Subscripts

C = coefficient
e = experimental
i = solid-gas interface
W = thermocouple wire
∞ = free stream

LITERATURE CITED

1. Bathish, L. N., and B. H. Sage, Document 6424, Am. Doc. Inst., Washington 25, D. C., $1.25 for photoprints or 35-mm microfilm.
2. Brown, R. A. S., Kazuhiko Sato, and B. H. Sage, *Ind. Eng. Chem., Chem. and Eng. Data Series*, **3**, 263 (1958).
3. Blasius, Heinrich, *Z. Angew. Math. u. Phys.*, **56**, 1 (1908); *Natl. Advisory Comm. Aeronaut. Tech. Memo 1256* (1950).
4. Cary, J. R., *Trans. Am. Soc. Mech. Engrs.*, **75**, 483 (1953).
5. Corcoran, W. H., J. B. Opfell, and B. H. Sage, "Momentum Transfer in Fluids," Academic Press, New York (1956).
6. Davis, Leo, *Rept. 3-22*, Jet Propulsion Laboratory, California Institute Technol., Pasadena (1950).
7. Davis, Leo, *Rept. 3-17*, Jet Propulsion Laboratory, California Institute Technol., Pasadena (1952).
8. Drake, R. M., Jr., *J. Aeronaut. Sci.*, **20**, 309 (1953).
9. Eckert, Ernst, *Forsch. Gebiete Ingenieurew., Forschungsheft No. 416*, 1 (1942).
10. Frössling, Nils, *Lunds Univ. Arsskr.*, N. F. Avd 2, Bd 36, Nr. 4 (1940); *Natl. Advisory Comm. Aeronaut. Tech. Memo 1432* (1958).
11. Hsu, N. T., and B. H. Sage, *A.I.Ch.E. Journal*, **3**, 405 (1957).
12. Hsu, N. T., Kazuhiko Sato, and B. H. Sage, *Ind. Eng. Chem.*, **46**, 870 (1954).
13. Johnstone, H. F., R. L. Pigford, and J. H. Chapin, *Trans. Am. Inst. Chem. Engrs.*, **37**, 95 (1941).
14. Korobkin, Irving, *Am. Soc. Mech. Engrs.*, Paper 54-F-18, Am. Soc. Mech. Engrs. Milwaukee Meeting (September, 1954).
15. Lautman, L. G., and W. C. Droege, Serial No. *AIRL A6118*, Air Materiel Command, 50-15-3 (August, 1950).
16. McAdams, W. H., "Heat Transmission," McGraw-Hill, New York (1954).
17. Pohlhausen, K., *Z. Angew. Math. u. Mech.*, **1**, 252 (1921).
18. Sato, Kazhuiko, and B. H. Sage, *Trans. Am. Soc. Mech. Engrs.*, **80**, 1380 (1958).
19. Schlichting, Hermann, "Boundary Layer Theory," McGraw-Hill, New York (1955).
20. Short, W. W., R. A. S. Brown, and B. H. Sage, *J. Appl. Mech.*, **27**, 393 (1960).
21. Short, W. W., and B. H. Sage, *A.I.Ch.E. Journal*, **8**, 1 (1960).
22. Sibulkin, Merwin, *J. Aeronaut. Sci.*, **19**, 570 (1952).
23. Tang, Y. S., J. M. Duncan, and H. E. Schweyer, *Natl. Advisory Comm. Aeronaut. Tech. Note 2867* (March, 1953).
24. Wadsworth, J., *Rept. MT-39*, National Research Council of Canada, Div. Mech. Engr. (September 12, 1958).
25. Xenakis, G., A. E. Amerman, and R. W. Michelson, *WADC Tech. Rept. 53-117*, Wright Air Development Center, Dayton, Ohio (April, 1953).

Manuscript received December 1, 1959; revision received April 5, 1960; paper accepted April 7, 1960.